

Non-thermal , High-energy, Laser-induced Nano-fusion



Radiative electro-magnetic (EM) energy transfer

Thermal or mechanical ? Possible both ways:

- Thermal: Black body radiation → loss & Carnot efficiency → Entropy current. Most fusion energy schemes assume thermal processes.
- “Mechanical”: Monochromatic conductors, Coaxial or Rectangular Wave guides, Lasers, Monochromatic (~~~) broadcast, near to 100% efficiency! (Directed radio (TV) broadcast possible to astronomical distances!)

Goal: Laser Induced Fusion Energy

- Transfer laser energy to nuclear reactions with minimal loss →
- **Non-thermal processes are preferred**
- E.g. convert laser energy to fusion target nuclei (p, d, t, He3, etc.) with **least possible loss**

Some early ideas for NanoTech Laser Induced Fusion Energy (NATLIFE)

Early nanotech trial example (2016):

Propagating sound waves *towards the cones* – less noise ~ no white noise (~ no black body r.) In concert halls no echo, minimal noise – absorbing all white noise → clear musical sound, directly from musical instruments



All incoming sound energy is absorbed, and thermalized and converted to heat in the wall-covers. Good example for ~100% energy absorption

& thermalization !

This was realized by Vural Kaymak et al. in 2016

[V. Kaymak, A. Pukhov, V. N. Shlyaptsev, J.J. Rocca, “Nanoscale ultradense Z - pinch formation from laser-irradiated nanowire arrays,” *Phys. Rev. Lett.* **117**, 035004 (2016).]

[Kaymak, V; Pukhov, A; Shlyaptsev, VN; Rocca, JJ, Strong ionization in carbon nanowires, *Quantum Electronics*, Vol. 46 (4) 327-331 (2016).]

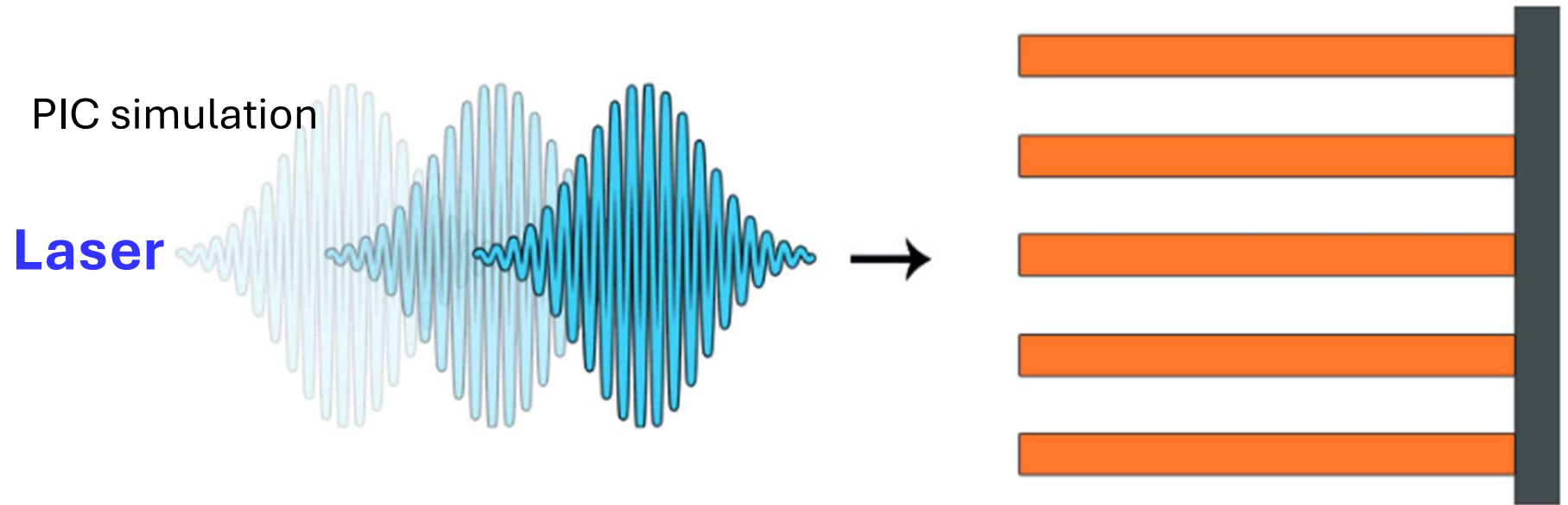
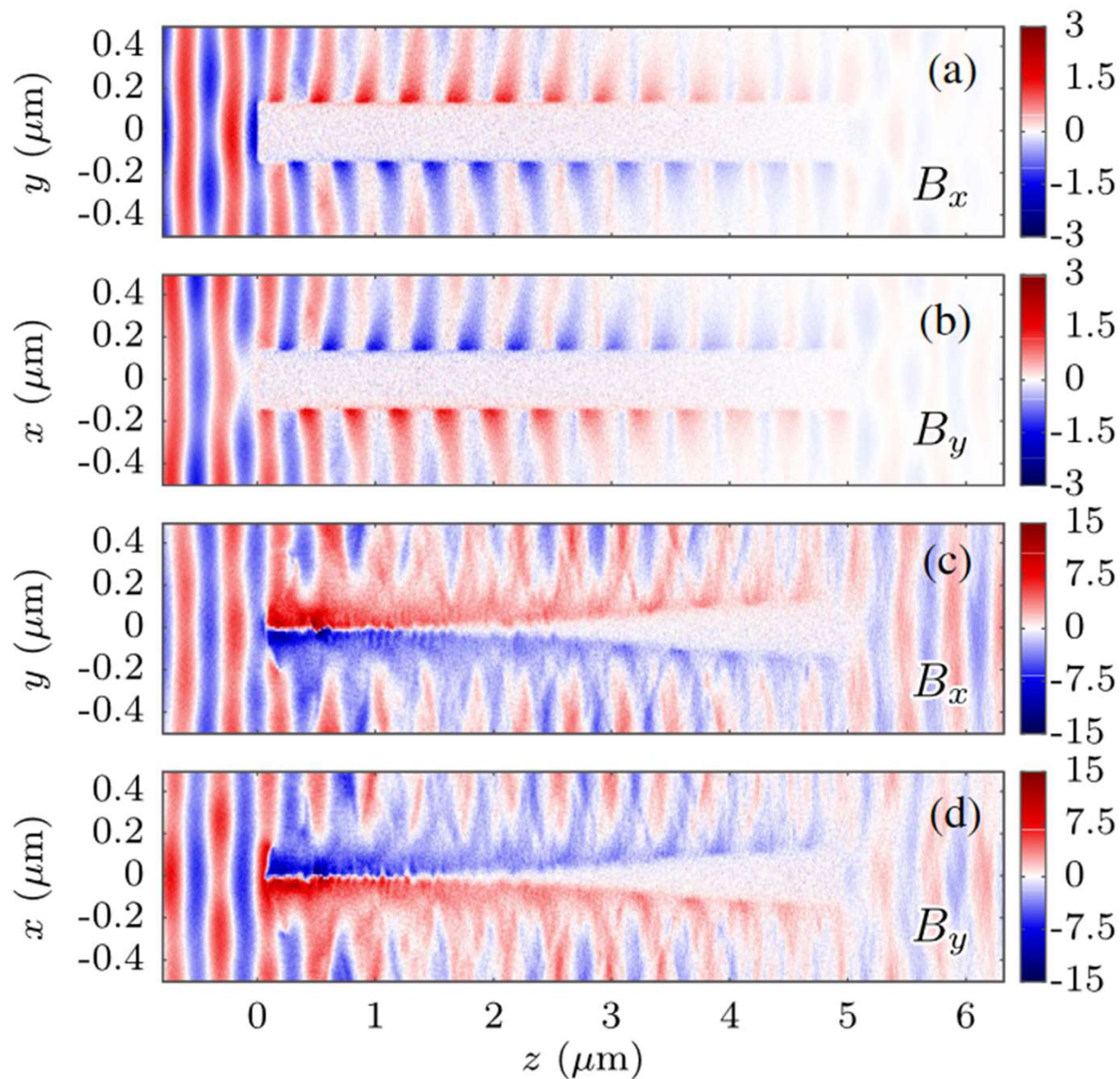


Figure 1. Scheme of the simulation setup.

E-field & e-resonance are polarized transversely to direction of radiation.

light ≠ sound !



[V.K. PRL (2016)] PIC
(Particle In Cell method)

Resonance, *transverse* to radiation (& **nano-wires**) is observed. Energy density of EM-field is absorbed inwards

L (length) \approx **5-7 μm**

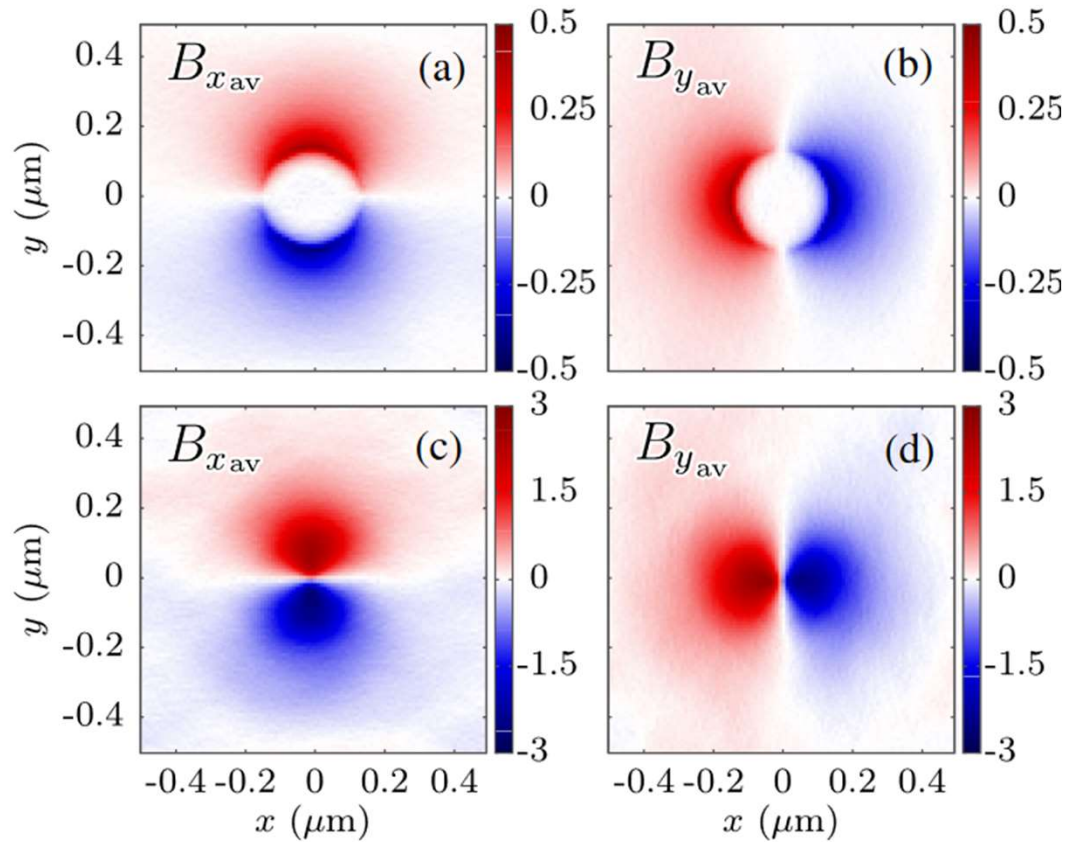
Width \approx **0.8 μm**

= 800 nm / in air !

FIG. 2. Longitudinal cross sections of magnetic field components B_x and B_y [in gigagauss (GG)] at (a),(b) $t = -35T_0$ and (c), (d) $t = -7T_0$. Laser propagation is from left to right.

T_0 is the Laser period ($T_0 = 1.33$ fs).

[VK PRL (2016)]



[V.K. ea PRL (2016)] PIC

FIG. 3. Quasistatic magnetic field components in GG at (a),(b) $t = -35T_0$ and (c),(d) $t = -7T_0$, where T_0 is the Laser period ($T_0 = 1.33$ fs). [VK PRL (2016)]

[C.B. & V.K. ea PRL (2017)] PIC

Clayton Bargsten, Reed Hollinger, Maria Gabriela Capeluto, Vural Kaymak, Alexander Pukhov, Shoujun Wang, Alex Rockwood, Yong Wang, David Keiss, Riccardo Tommasini, Richard London, Jaebum Park, Michel Busquet, Marcel Klapisch, Vyacheslav N. Shlyaptsev, Jorge J. Rocca, Energy penetration into arrays of aligned nanowires irradiated with relativistic intensities: Scaling to terabar pressures, *SCIENCE ScienceAdvances* **3** (1) e1601558 (2017). [CA&VK SA (2017)].

[C.B. ea (2017)]

A

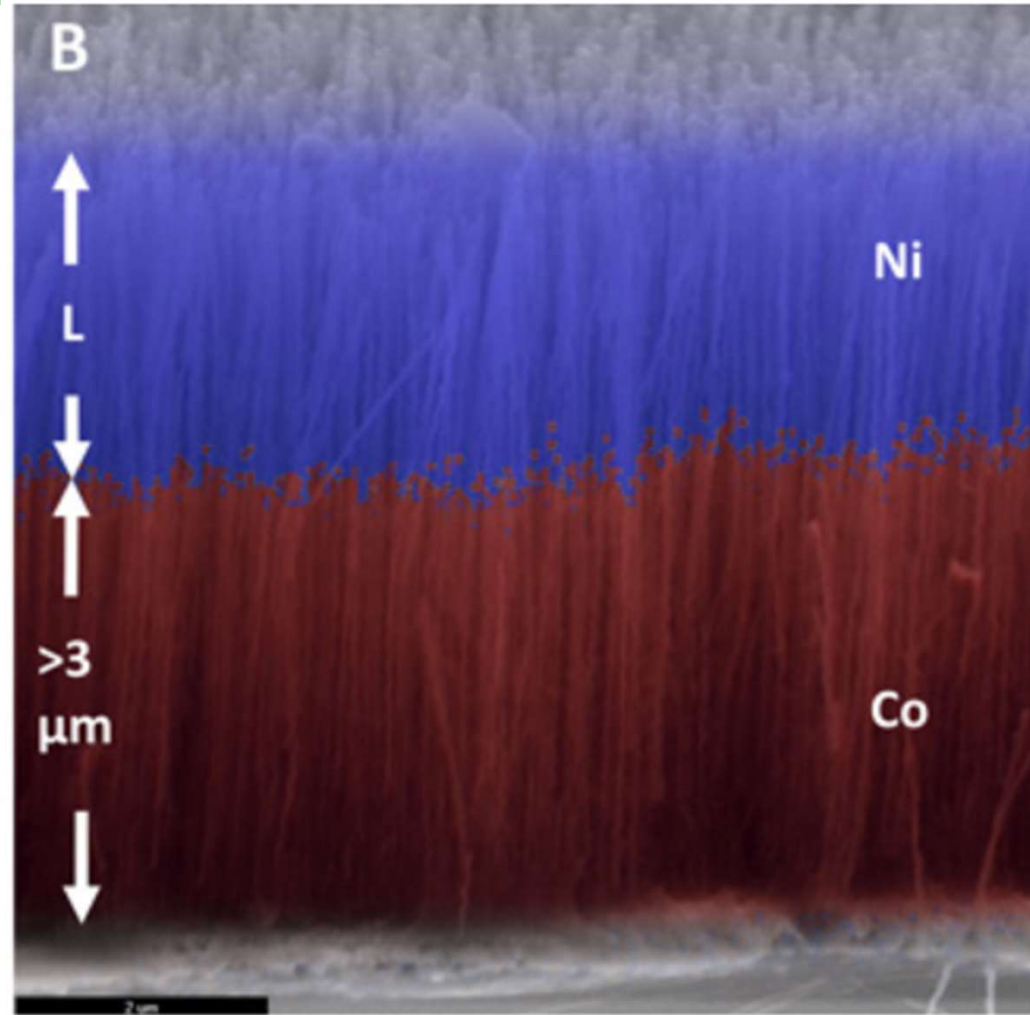
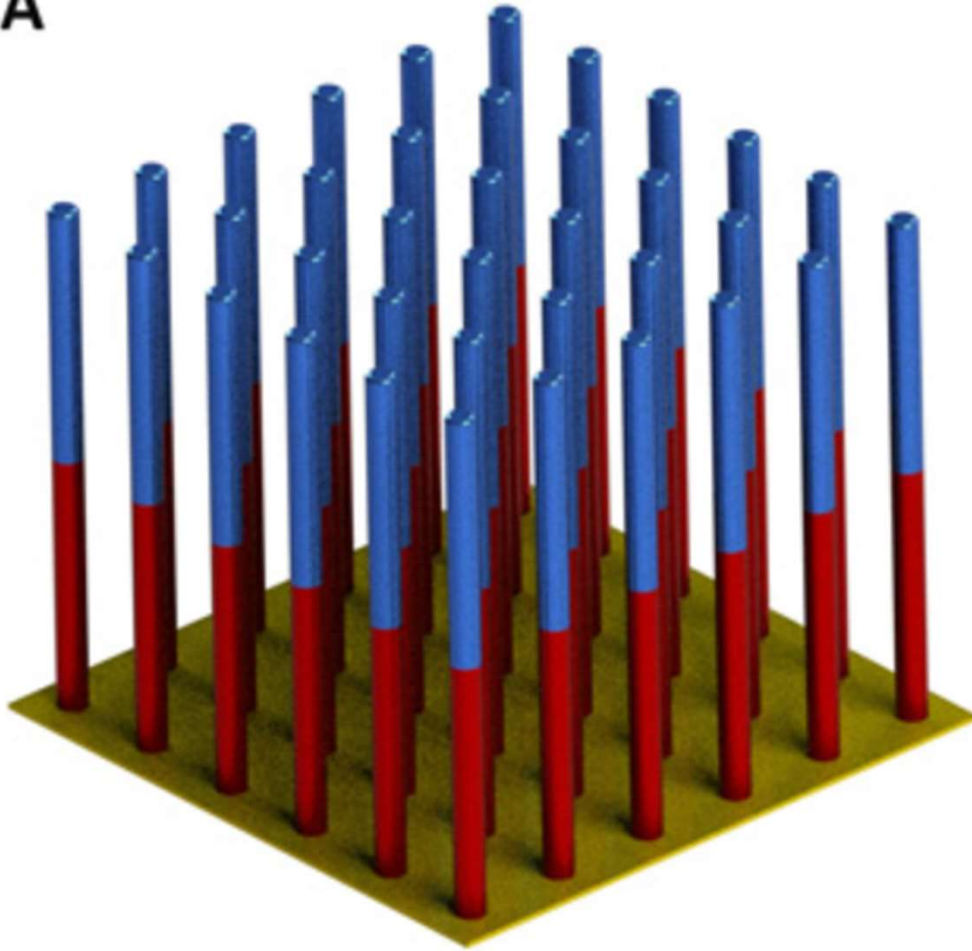
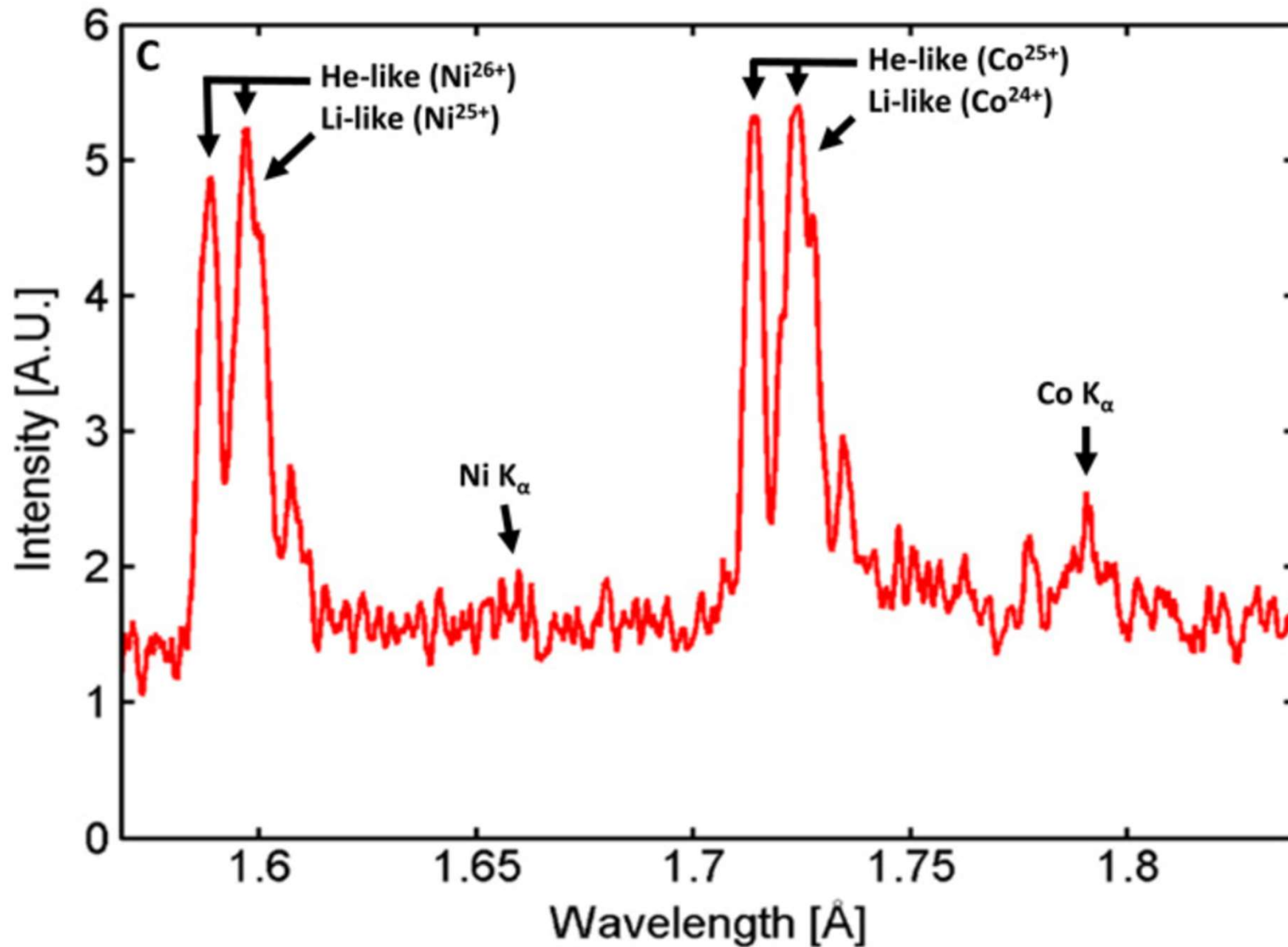


Fig. 1 Schematic diagram, composition map, and x-ray spectrum of a two-composition Ni-Co nanowire array.

(A) Schematic diagram of segmented two-composition Ni-Co nanowire array. The top Ni segment ranges in length from 1 to 6 μm . The nanowires are **55 nm in diameter** and form an array that is 13% of solid density. (B) Scanning electron microscopy **image** with energy-dispersive spectroscopic elemental composition measurement indicating the concentration of Ni (blue) and Co (red). [CB ScA (2017)]⁸



[C.B. ea
(2017)]

(C) Example spectra showing the He-like line dominance over the K_α lines for the two elements as recorded using a von Hamos crystal spectrometer. A.U., arbitrary units.

[CB ScA (2017).]

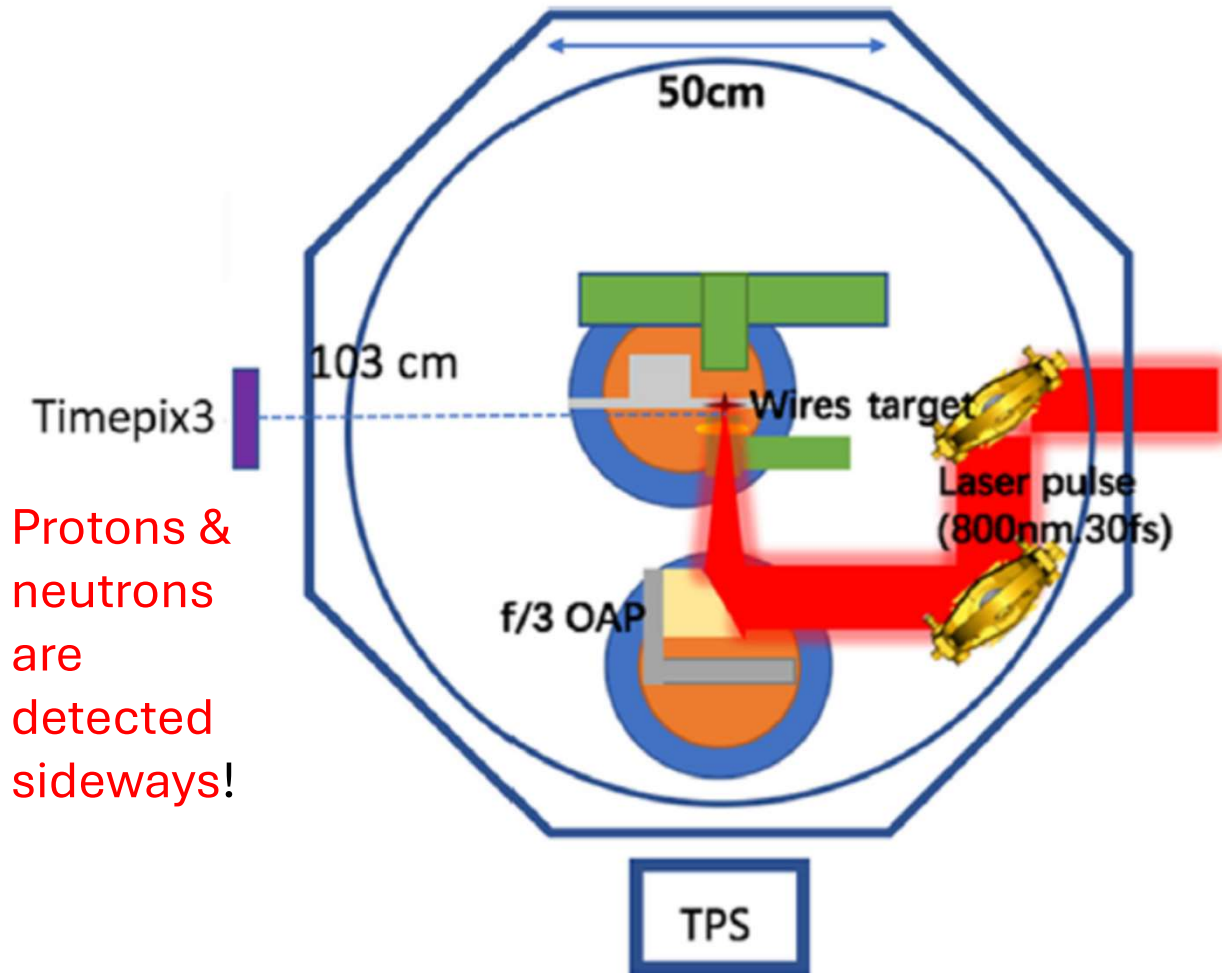
Recent publications:

Peter Rubovič, Aldo Bonasera, Petr Burian, Zheng Xuan Cao, Changbo Fu, Defeng Kong, Haoyang Lan, Yao Lou, Wen Luo, Chong Lv, Yugang Ma, Wenjun Mae, Zhiguo Ma, Lukáš Meduna, Zhusong Mei, Yesid Mora, Zhuo Pan, Yinren Shou, Rudolf Sýkora, Martin Veselský, Pengjie Wang, Wenzhao Wang, Xueqing Yan, Guoqiang Zhang, Jiarui Zhao, Yanying Zhao, Jan Žemlička,
Measurements of D–D fusion neutrons generated in *nanowire array* laser plasma using Timepix3 detector, *Nuclear Inst. and Methods in Physics Research A*, **985**, 164680 (2021). [PRAB NIM (2021)]

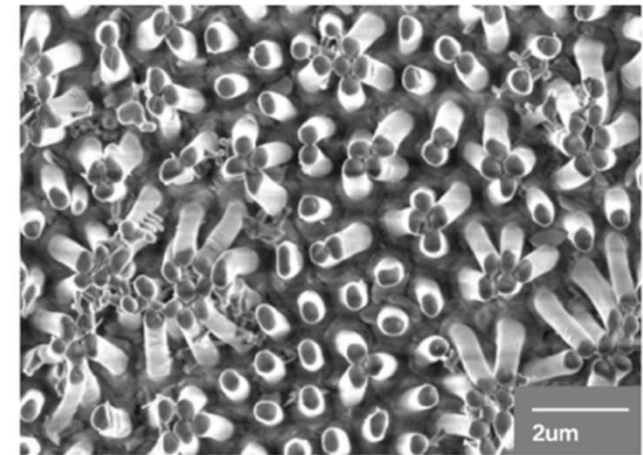
Defeng Kong, Guoqiang Zhang, Yinren Shou, Shirui Xu, Zhusong Mei, Zhengxuan Cao, Zhuo Pan, Pengjie Wang, Guijun Qi, Yao Lou, Zhiguo Ma, Haoyang Lan, Wenzha Wang, Yunhui Li, Peter Rubovic, Martin Veselsky, Aldo Bonasera, Jiarui Zhao, Yixing Geng, Yanying Zhao, Changbo Fu, Wen Luo, Yugang Ma, Xueqing Yan, Wenjun Ma;
High-energy-density plasma in femtosecond-laser-irradiated nanowire-array targets for nuclear reactions, *Matter Radiat. Extremes* **7**, 064403 (2022).

Jorge J. Rocca, Maria G. Capeluto, Reed C. Hollinger, Shoujun Wang, Yong Wang, G. Ravindra Kumar, Amit D. Lad, Alexander Pukhov, & Vyacheslav N. Shlyaptsev, Ultra-intense femtosecond laser interactions with *aligned nanostructures*, *Optica*, **11** 437 (2024). [Rocca Op (2024)]

[PR AB ea 2021]



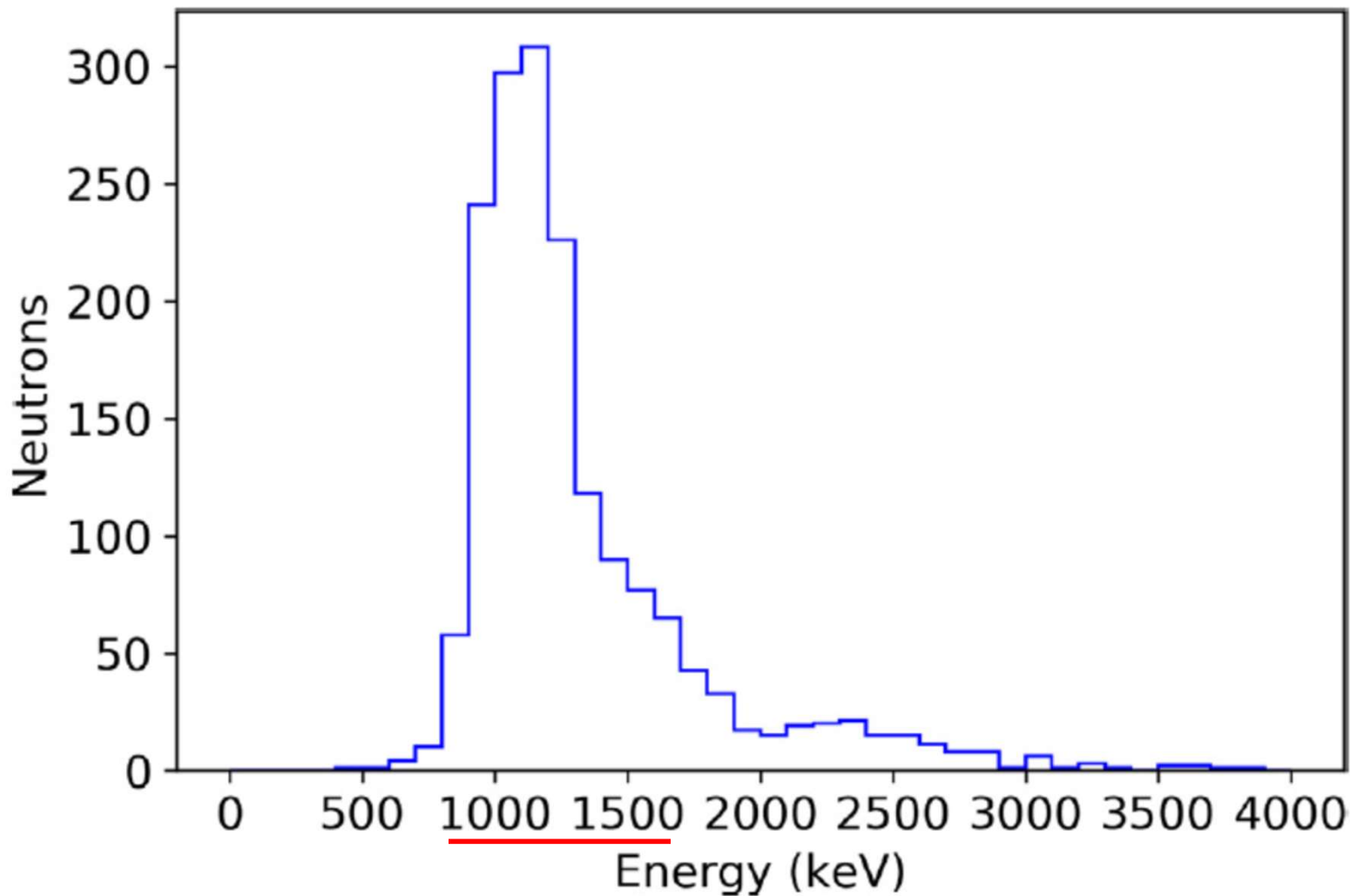
CD_2 nanowire array targets, the thickness of the **substrate** supporting the nanowire arrays is $\sim 500 \mu\text{m}$.



The image of the DPE nanowire array target with 500 nm diameter, 800 nm spacing and 5 μm length.

Fig. 1. The layout of the experimental chamber as described in the text. TPS stands for Thomson parabola spectrometer.

Spacing & $d \sim \lambda$; $L \sim 10 \lambda$
in UDMA: $\lambda/2 \sim 85 \text{ nm}$



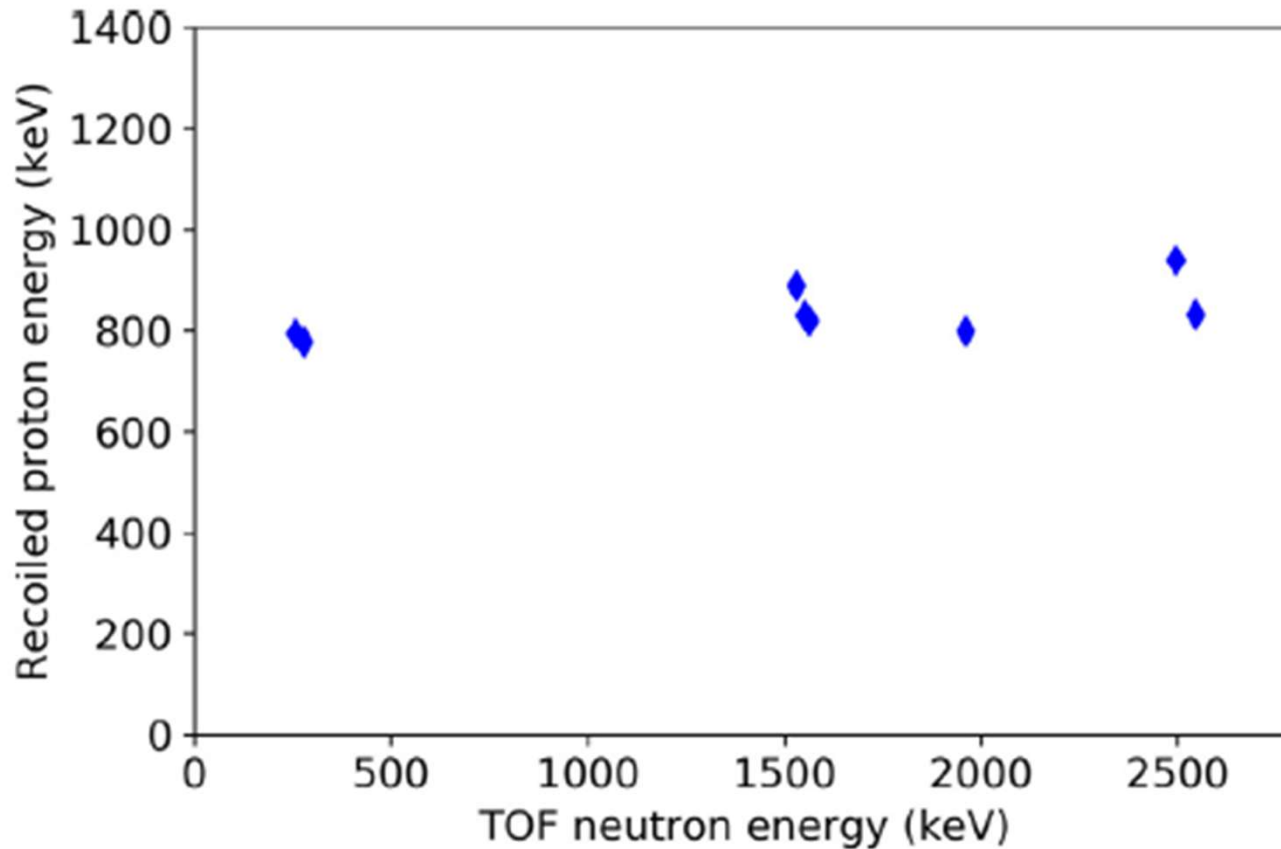
[PR AB ea
2021]

Proton formation
and acceleration
via incoming
neutrons

Resonant
features are
observed but not
recognized or
exploited

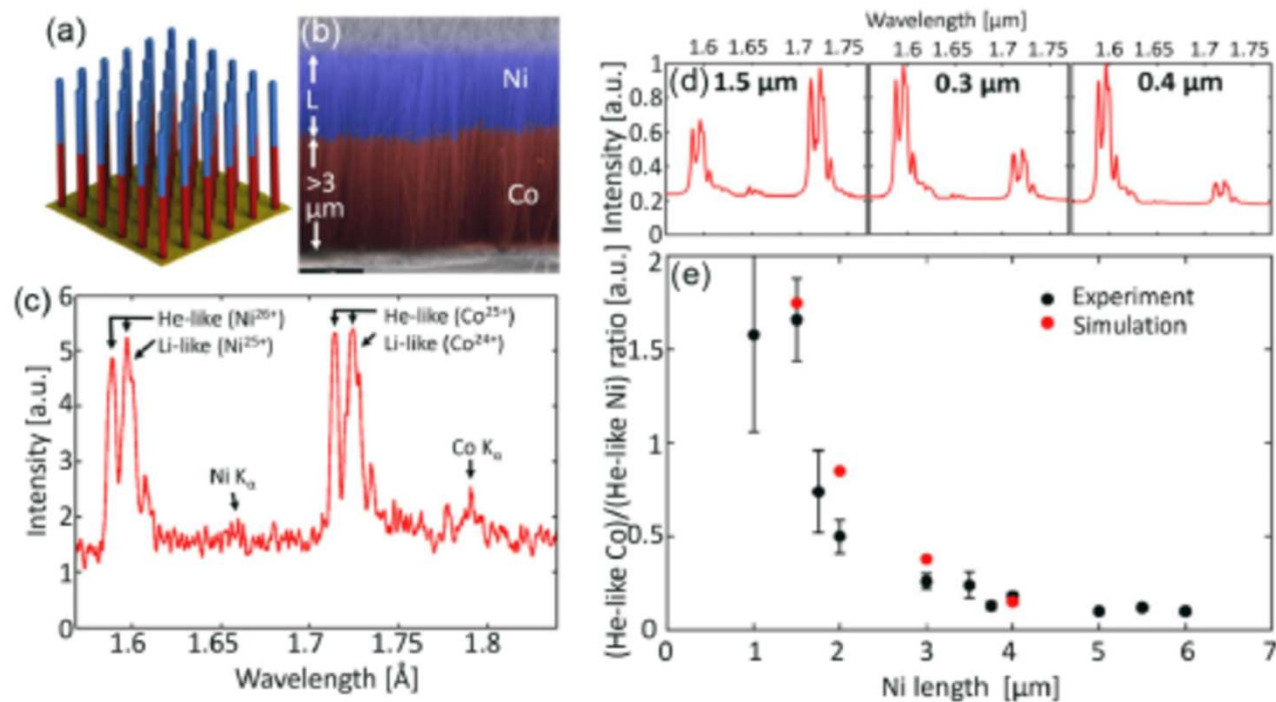
Fig. 9. The energy spectrum of recoiled protons from the measurement with 2.5 MeV neutrons generated with VdG accelerator.

[PR AB ea 2021]



Neutrons from D-D fusion are observed. Their energy is estimated via energy of generated protons..

Fig. 12. Plot of neutron energies derived from TOF measurements versus recoiled protons energy measured directly by Timepix3 detector.

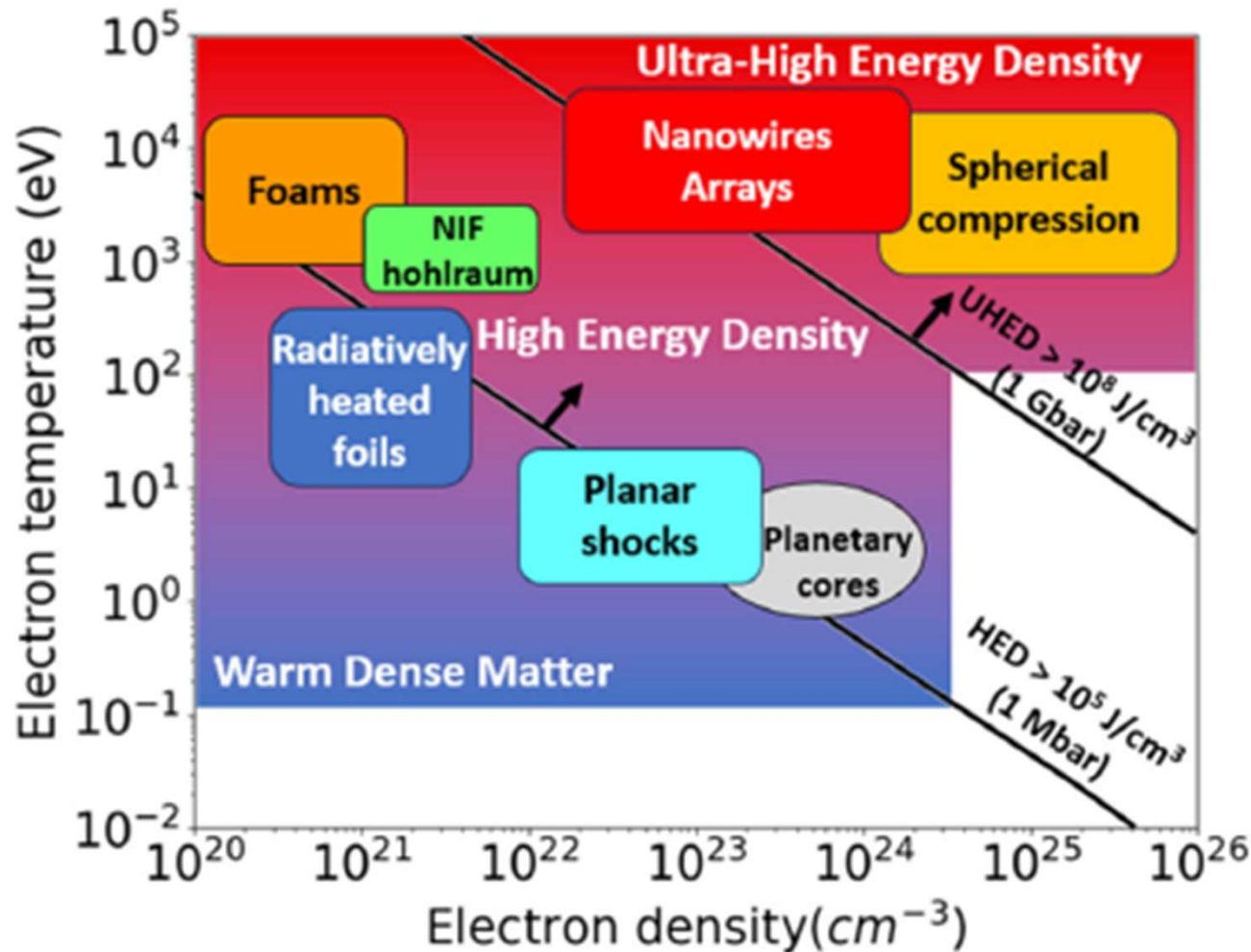


[Rocca ea 2024]

V Kaymak ea 2016 repeated
(e) Measurement is new

Fig. 3. (a) Schematic diagram of segmented Ni-Co nanowire array. The top Ni segment ranges in length from 1 to 6 μm. The nanowires are 55 nm in diameter and the array has 13% solid density. (b) Scanning electron microscope (SEM) image with energy-dispersive spectroscopic elemental composition measurement, indicating the concentration of Ni (blue) and Co (red). (c) Example spectra showing the He-like lines' dominance over the K_α lines for the two elements, as recorded with a von Hamos spectrometer. (d) Simulated spectra corresponding to the three arrays with different Ni wire segment lengths. (e) Measured and simulated (Co He-α)/(Ni He-α) line ratios as a function of the Ni nanowire segment length. Adapted from [49]. © The Authors, some rights reserved, exclusive licensee AAAS. Distributed under a Creative Commons Attribution NonCommercial License 4.0 (CC BY-NC) <http://creativecommons.org/licenses/by-nc/4.0/>. Csernai

[Rocca ea 2024]



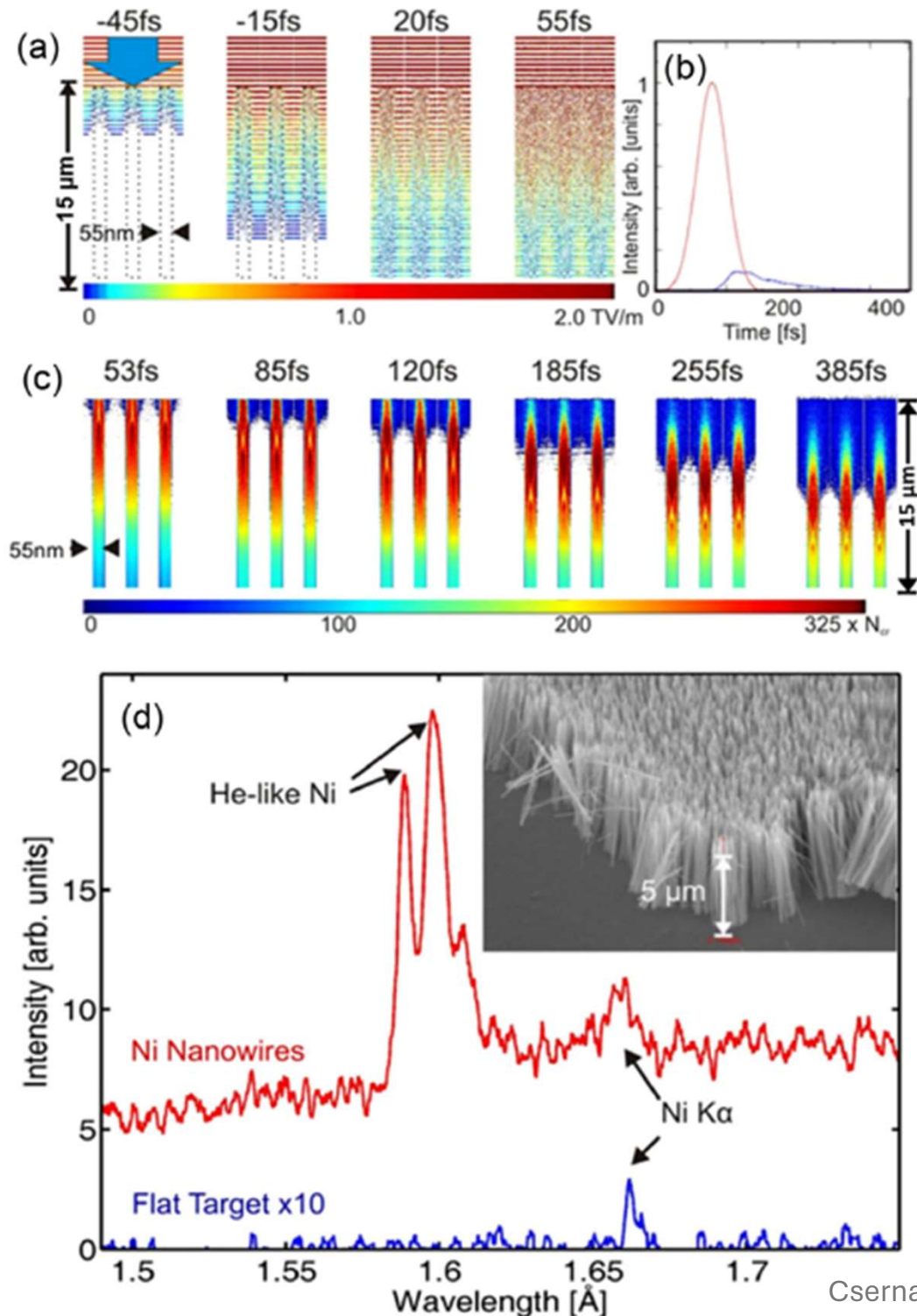
Summary (adapted)
Still in terms of
**temperature &
pressure !**

→

**Nanowire arrays are
advantageous**

Fig. 1. Plasma parameter space showing the typical parameters of plasmas generated by irradiating NW targets with femtosecond pulses of relativistic intensity relative to other high energy density plasmas. The black lines show the approximate limit of the region commonly accepted as high energy density (HED), $>1 \times 10^5 \text{ J cm}^{-3}$ and that defined as ultra-high-energy density (UHED), $>1 \times 10^8 \text{ J cm}^{-3}$. Adapted from [4] with permission from Springer Nature.

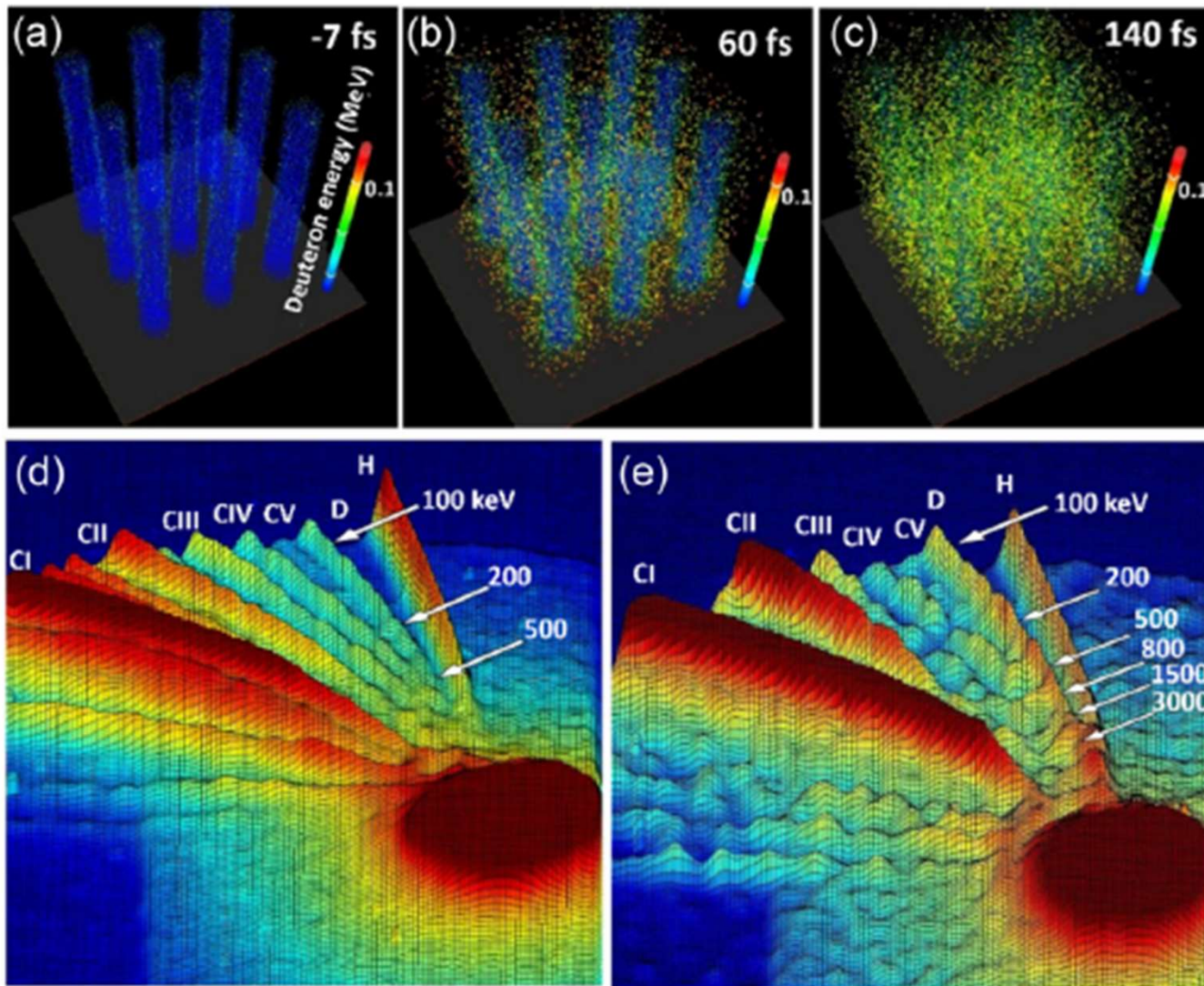
[Rocca et al 2024]



“NWs present a greatly increased effective absorption area to the laser beam. This allows the laser electric field to pull a much larger number of electrons from the NW surfaces, which are accelerated in the voids”. (55 nm $\sim \lambda_{\text{eff}}$)

Some part of resonance effects are observed (gap size).

[Rocca et al. 2024]



PIC simulated

“Thomson parabola” results are shown. H and D lines are visible and strong. Results are depending on irradiation time.

(See Papp et al. e & p kinetic energy spectra.)

Experimental detection setup is here not presented.

Fig. 10. (a)–(c) 3D PIC simulation of energy distribution of energetic deuterons at different times, in an array of 400 nm diameter CD₂ NW 16% of solid density irradiated at an intensity of $8 \times 10^{19} \text{ W cm}^{-2}$ by laser pulses of 60 fs duration. Times are measured with respect to the peak of the laser pulse. (d) Measured single-shot Thomson parabola ion energy spectra for a flat target (e) and for a CD₂ NW target. Reproduced with permission from [145].

[NAPLIFE -ELI-ALPS 2024] preliminary

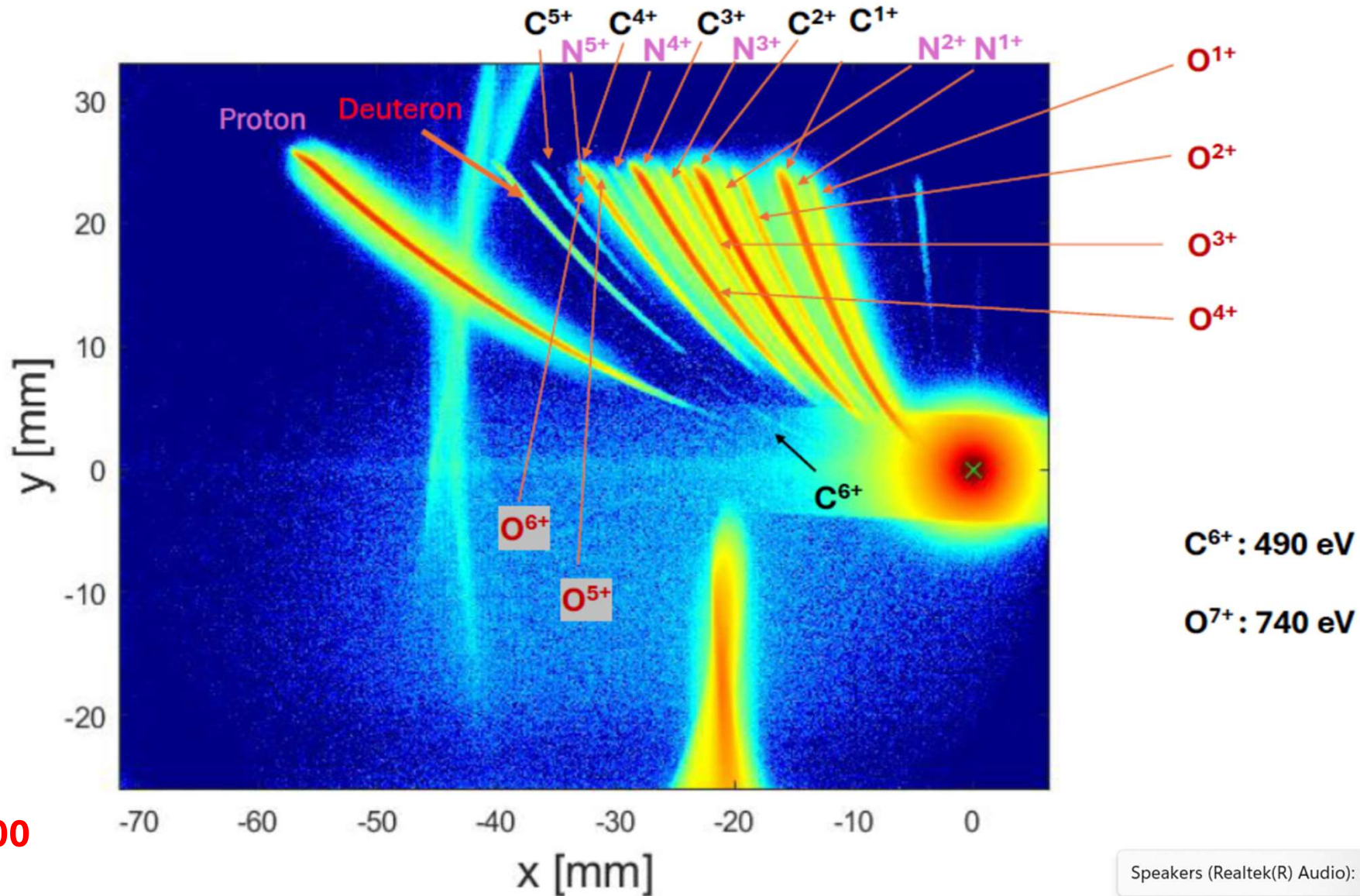
D100 sample

>100 spectra
are averaged

UDMA (urethane
dimethacrylate),
 $C_{23}H_{38}N_2O_8$

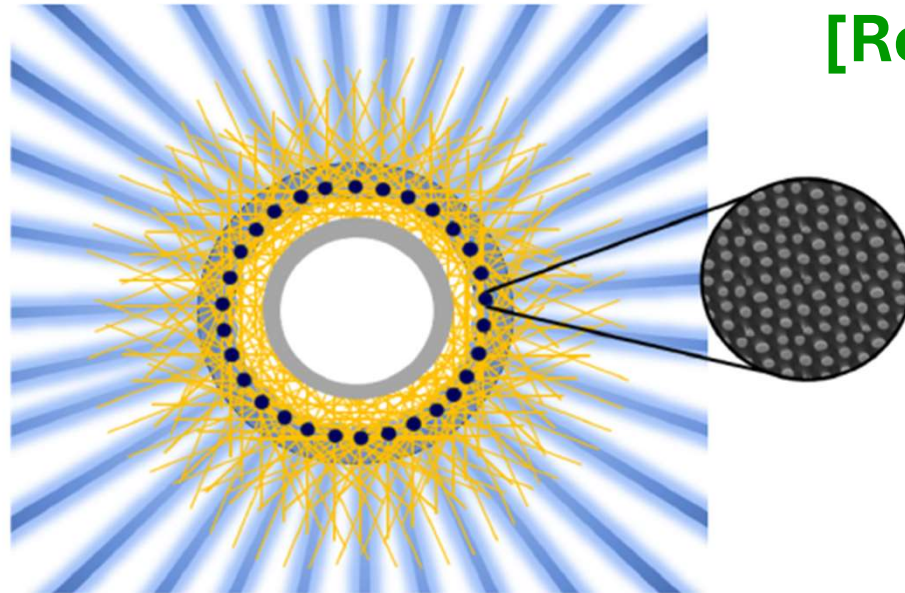
MMA (Methyl
methacrylate),
 $C_5H_8O_2$

MMA-D (Methyl-
 d_3 methacrylate-
 d_5), $C_5D_8O_2$ = **D100**



Speakers (Realtek(R) Audio): 4

Realization plan – Thermal / NIF TYPE - spherical, isotropic *cylindrical arrangement*



[Rocca ea 2024]

- Spherical shell fusion target
- Surrounded by nanowires
- Random isotropic ion flux (yellow)
- Fusion is thermal

Fig. 14. Schematic diagram of a 2-D fusion reactor concept in which an array of intense femtosecond laser pulses (blue beams) irradiates a target composed of embedded nanorods to efficiently accelerate a stream of ions to 0.1–2 MeV energies. The yellow lines are the ion trajectories. Ions impinge on a fuel shell (gray). The same concept can also be implemented using a 3-D configuration. A cylindrical fuel shell is included for illustration purposes. Inspired by Fig. 1 from [168].

Summary of the long nanowire expectations & results

- Long nanowires are parallel with the direction of laser irradiation
- Long nanowires increase laser light absorption & eliminate reflection
- Observed that nanowire diameter and spacing of the order of laser wavelength is enhancing their effect
- Observed that increased irradiation time (up to ~40 irradiation period) is increasing their effect

Differences

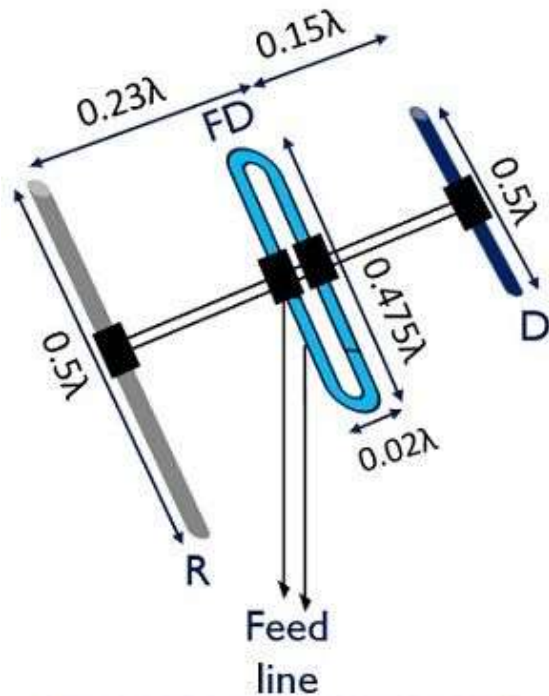
- The length of nanowires is more than an order of magnitude longer than the wavelength
- Possibility to **exploit resonant sizes** is not recognized
- **Polarization of the laser light** is not recognized and not exploited
- Change of **resonant sizes** due to materials and to aspect ratios are not recognized and not exploited

How can we explain that still these nanowires work (somewhat) ???

- **Nanowire array** --- **equivalent to** --- **Long Yagi-Uda antenna**

The Yagi-Uda antennas (in short Yagi-antennas) 1926

- The single thin wire resonant dipole antenna can receive EM broadcast even from weak signal and considerable noise. Then the received signal can be led to the receiver with a cable (e.g. coaxial or other type)
- **Yagi H.** and **Uda S.** increased the efficiency of these antennas in **1926** by adding director and reflector elements to the dipole.

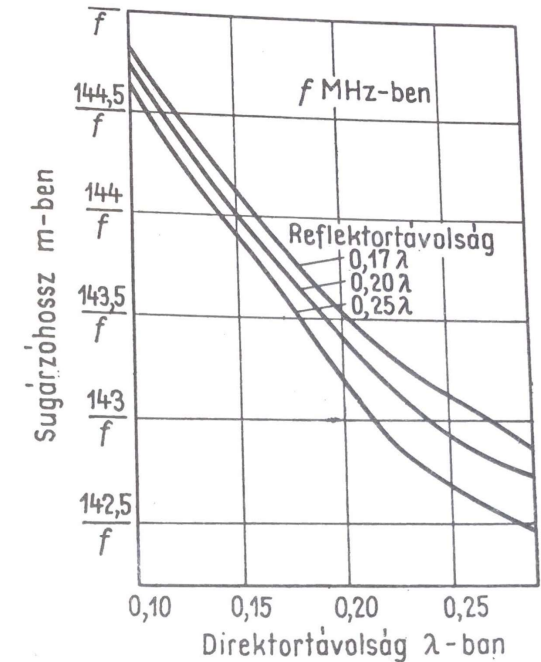


Yagi Antenna

Electronics Desk

[K. Rotamer:
Antennenbuch,
Deutscher Militärverlag,
Berlin (2017)]

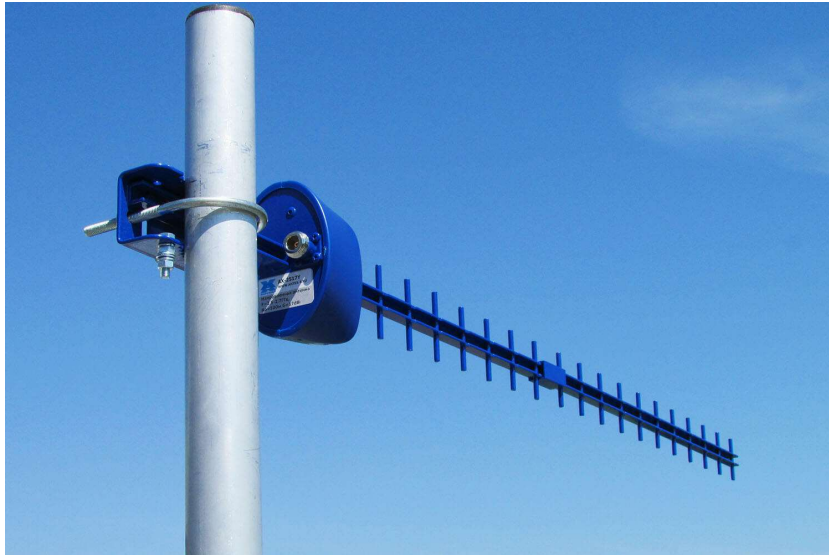
**For us no feed line and
no looped dipole are
needed!**



16.7. ábra. A háromelemes Yagi-antenna táplált elemének hossza a direktor és a reflektor távolságának függvényében

Long Yagi antennas with many directors

Equivalent to **one** “velvet” nano-wire rod used for good absorption



Length $\approx 10 \lambda = 5-6 \mu m$

Transverse size

$\approx 0.4-0.5 \lambda = 0.01 \mu m$

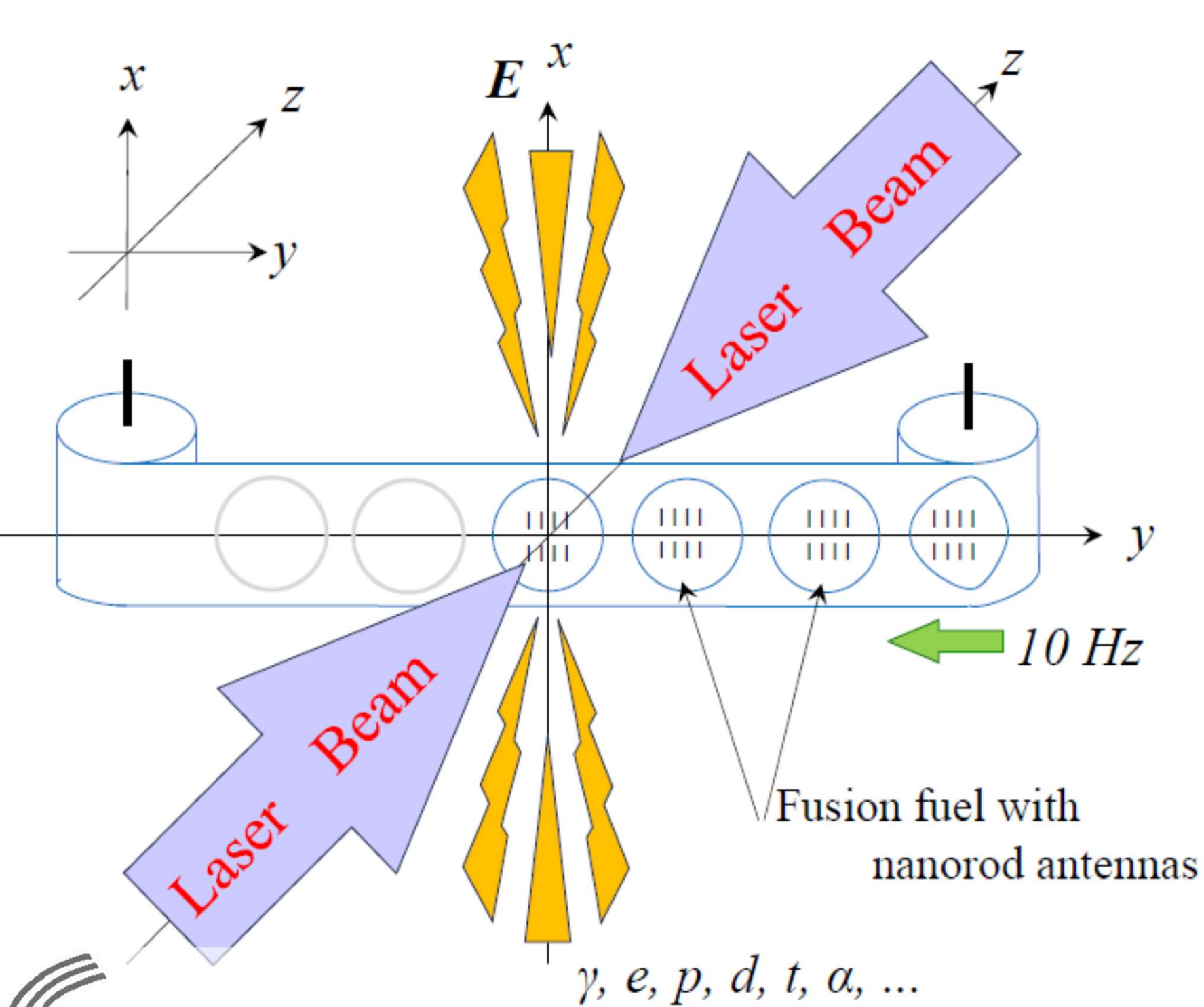


Butterfly \Leftrightarrow increased Band width

Stacked Yagi antennas ~ Nanowire arrays



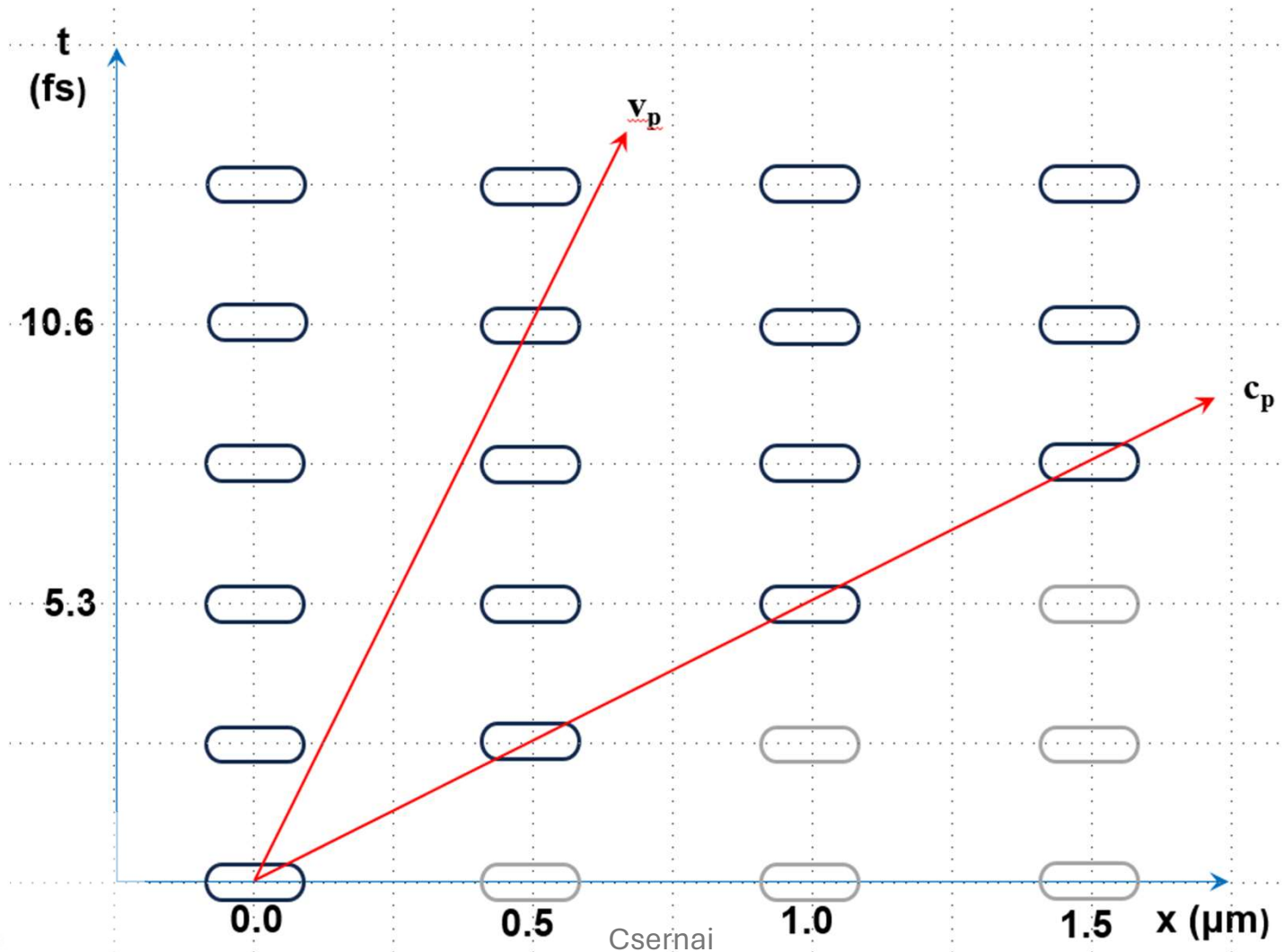
- We do not need “FEED Line”,
- We want to **accelerate protons or deuterons,**
- In the direction of the dipoles
- With two-sided laser irradiation



Industrial setup

Distance between Yagi-type antenna array columns

Director distance should be such that the protons/deuterons are reaching the next array when that is in the phase, which accelerates it further.





Laser wake field collider

NAPLIFE Collaboration

István Papp^{a,b,*}, Larissa Bravina^c, Mária Csete^d, Igor N. Mishustin^{e,f}, Dénes Molnár^g, Anton Motornenko^e, Leonid M. Satarov^e, Horst Stöcker^{e,h,i}, Daniel D. Strottman^j, András Szenes^d, Dávid Vass^d, Tamás S. Biró^a, László P. Csernai^{a,b,e}, Norbert Kroó^{a,k}

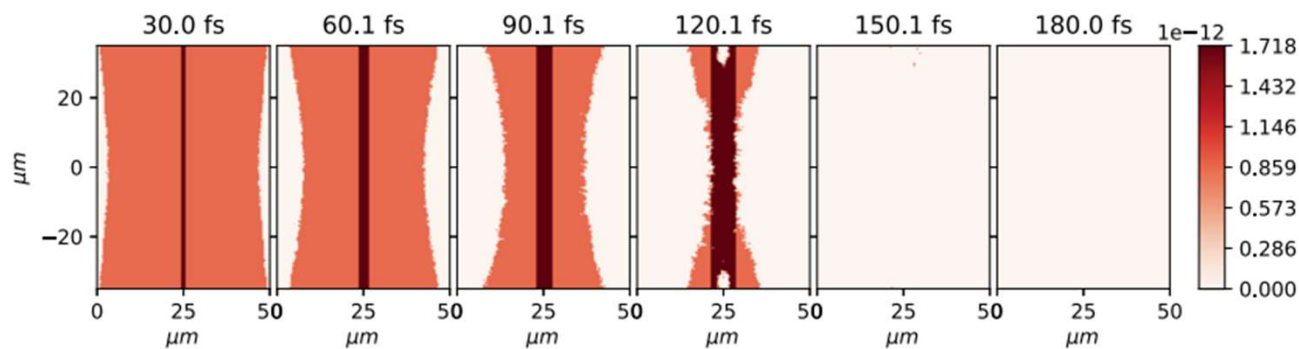
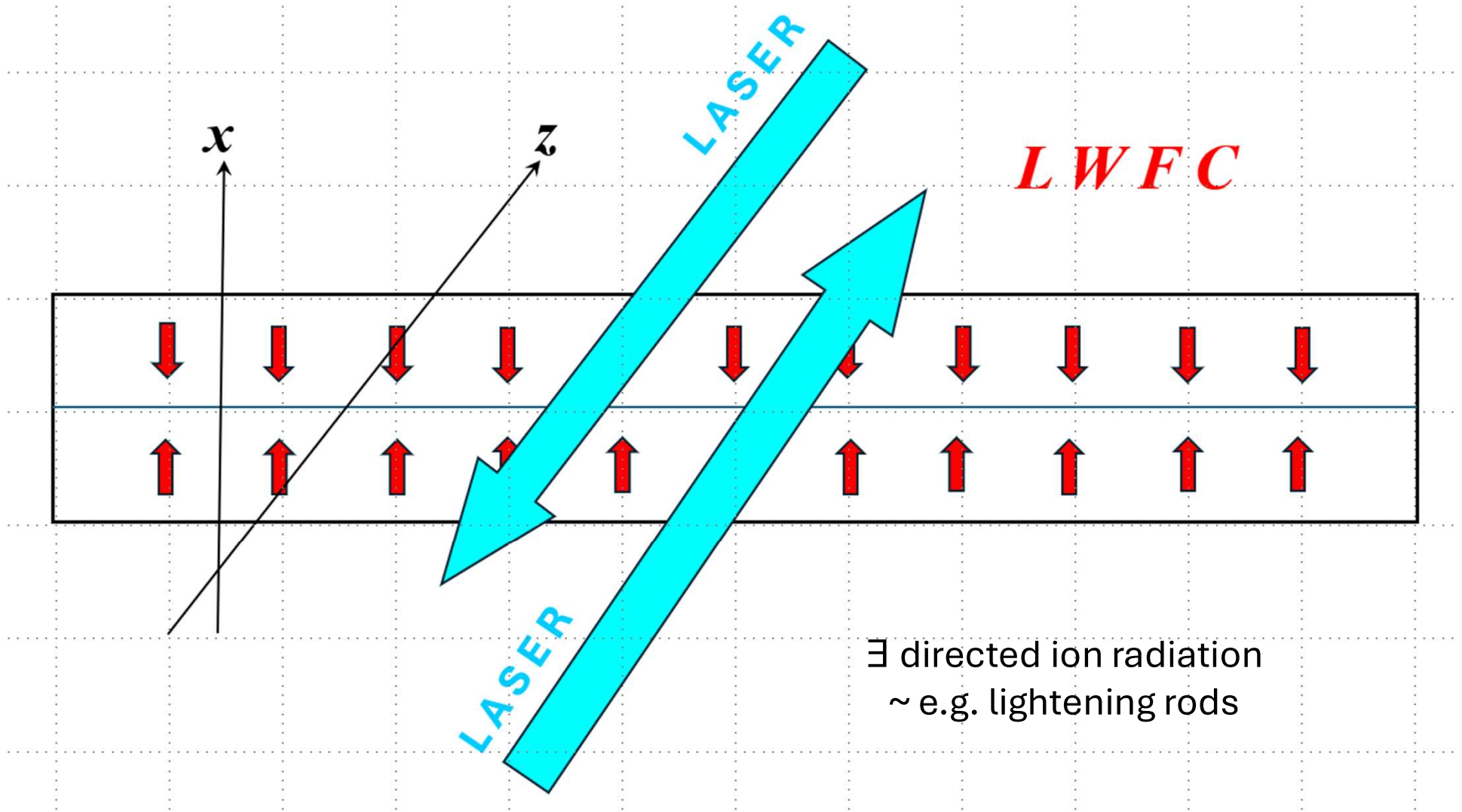
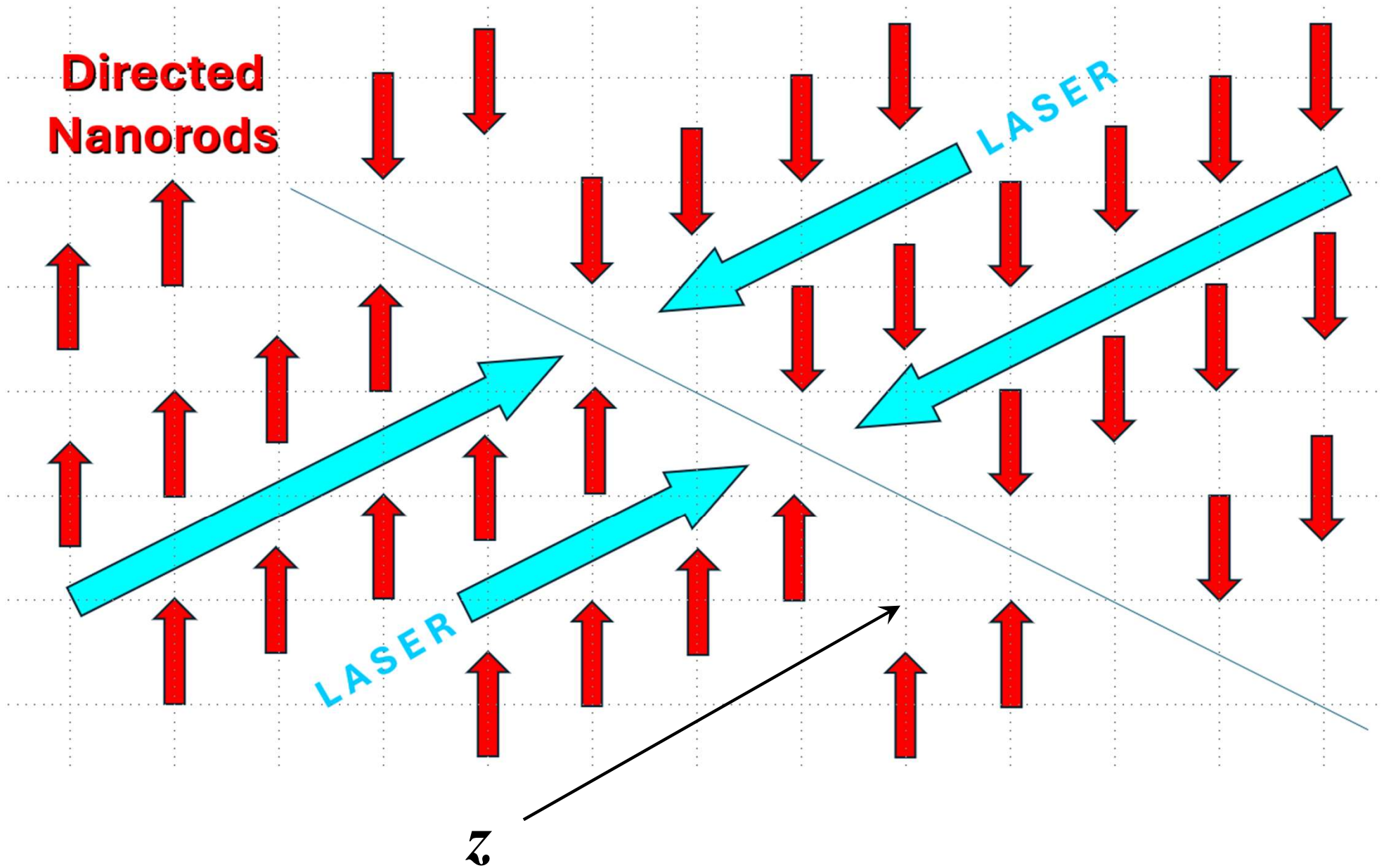


Fig. 2. (Color online) The ionization of the H atoms in a Laser Wake Field (LWF) wave due to the irradiation from both the $\pm x$ -directions, on an initial target density of $n_H = 2.13 \cdot 10^{27}$ atoms/m³ = $2.13 \cdot 10^{21}$ atoms/cm³. The energy of the H atoms in Joule [J] per marker particle is shown. The H atoms disappear as protons and electrons are created. Due to the initial momentum of the colliding H slabs, the target and projectile slabs interpenetrate each other and this leads to double energy density. Several time-steps are shown at 30 fs time difference.



\exists directed ion radiation
 ~ e.g. lightning rods

- Laser beam from $\pm z$ direction
- Nanorod antennas pointing to $\pm x$ direction
- Flat fusion fuel target is in the $[x - y]$ plane



**Directed
Nanorods**

LASER

LASER

z

Directors & Dipoles in the z direction

Laser Wake Field Collider

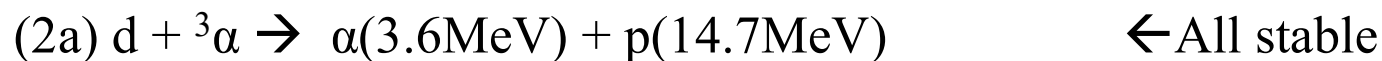
non-spherical, non-thermal, **not NIF TYPE**

- Deuterons, (protons, 3He ions, ...) can be accelerated in **one direction** (not thermalized !!!).
- Two such colliding beams with full energy may lead to **higher energy nuclear fusion reactions**, with higher reaction rate.
- In the x (E-field) direction two slabs (/w evt gap) on top of each other accelerated towards each other with non-thermal speed. The materials of the two slabs may be different, e.g. Deuteron + He^3

Nuclear reactions

Notations:

${}^1_1\text{H} := \text{p}$ Proton, ${}^2_1\text{D} := \text{d}$ Deuteron, ${}^4_2\text{He} := \alpha$, ${}^3_2\text{He} := {}^3\alpha$, ${}^3_1\text{T} := \text{t}$ Tritium (12y)



${}^3_2\text{He}$ abundance is 0.0002%

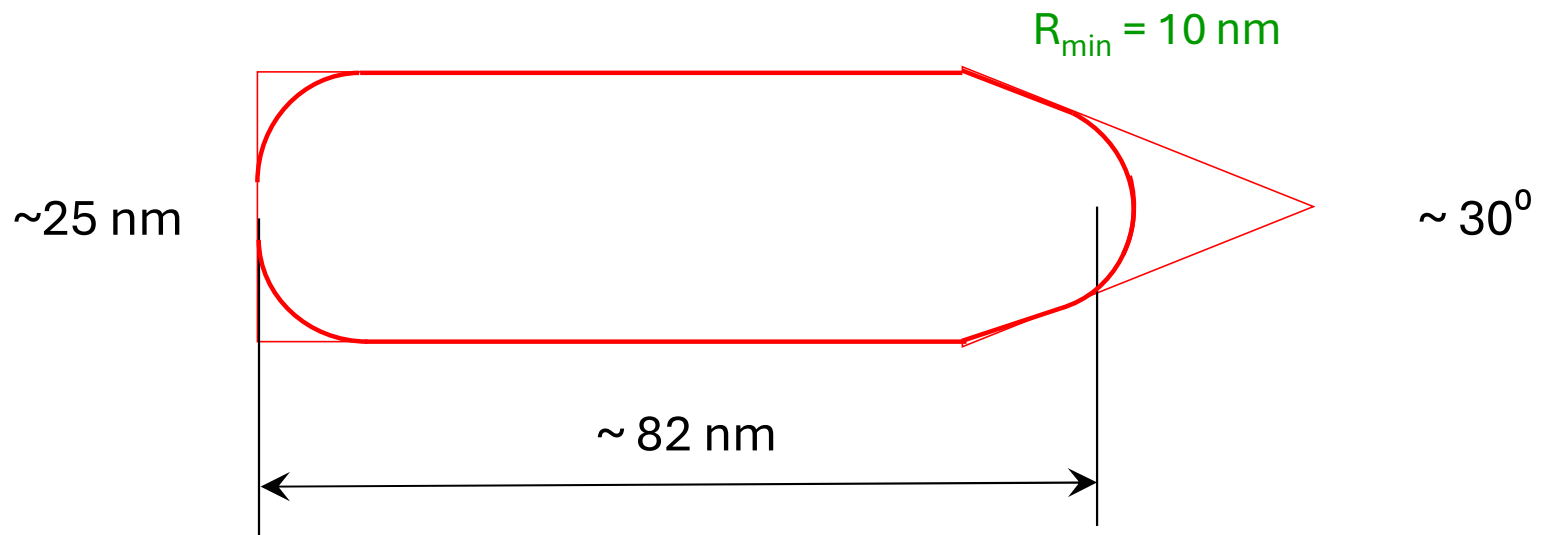
Mining it on the Moon !?

The *primary* reaction (1) may be non-thermal !! $A+B \rightarrow c+d$ *secondary* reactions at ~ 100 keV energy, have isotropic c. s. (At MeV\GeV energies are forward peaked.)

Thanks for your attention

Directed dipole nanorod antenna for proton emission in one direction

For sharp resonance at $\lambda = 795 \text{ nm}$



Possible electron lithography target materials:

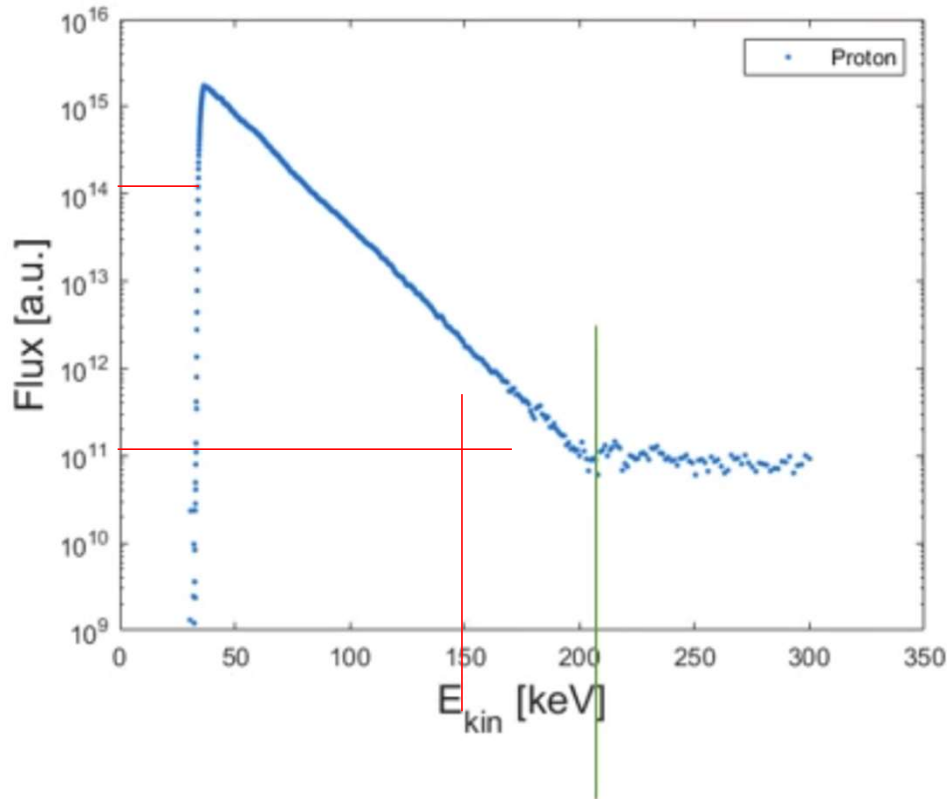
Resist: Deuterated polystyrene w/ resonant golden nanoantennas

Substrate: Glass

NAPLIFE @ ELI – ALPS Deuterized target without/with Au Nanoantennas

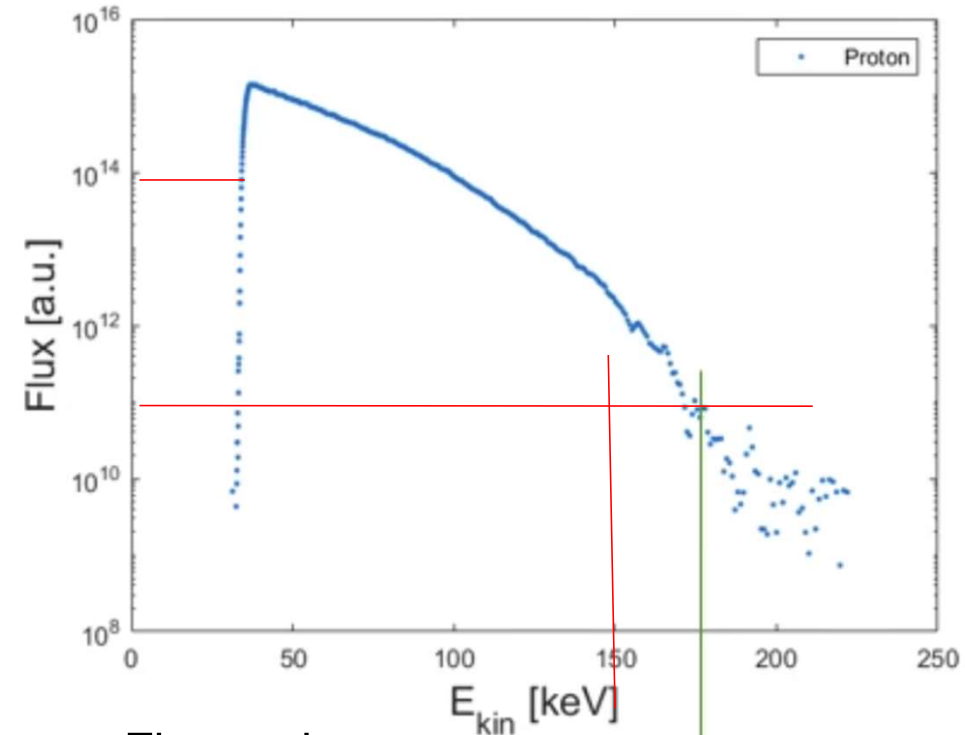
Proton emission

D100

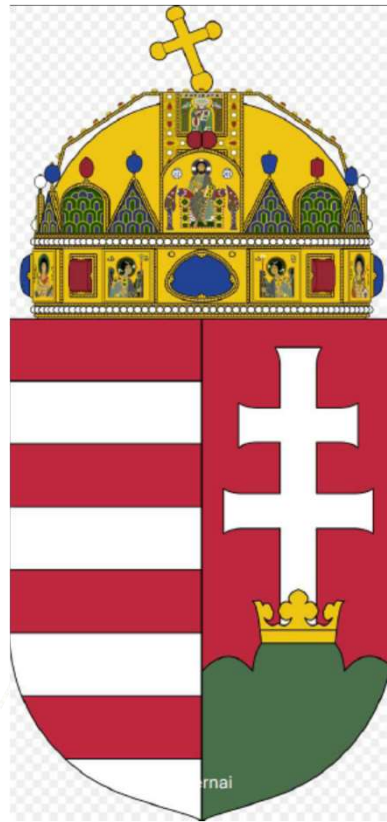
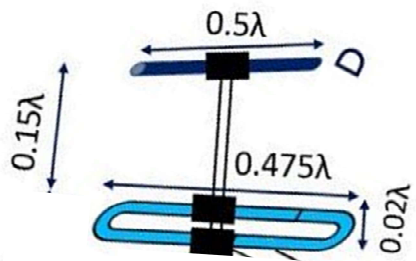


Exact – thermal
distribution
“Fireball model”

D100 Au2 resonant



Thermal +
collective expansion flow
[Siemens & Rasmussen, PRL 42, 880 (1979),
Siemens & Kapusta, PRL 43, 1690 (1979).]
“ Blast-wave model”



Simple Yagi
antenna with one
director and one
dipole (& long
axis holder)

Sizes in vacuum:

$\lambda \approx 0.8 \mu\text{m} = 800 \text{ nm}$, $\lambda/2 \approx 0.4 \mu\text{m} = 400 \text{ nm}$, thick antenna is shorter by 5%
Long, multi-director antenna length $\sim 10 \lambda = 5 \text{ \ } 8 \mu\text{m}$, $w \cdot h = 0.4 \text{ \ } 0.1 \mu\text{m}$
Gap $g = \lambda/10 \approx 0.08 \mu\text{m} = 80 \text{ nm}$

Sizes in UDMA:

$\lambda/2 \approx 0.08 \mu\text{m} = 80 \text{ nm}$, thick antenna
Long, multi-director antenna length $\sim 10 \lambda = 2 \mu\text{m}$, $w \text{ \ } h = 0.08 \text{ \ } 0.02 \mu\text{m}$
Gap $g = \lambda/10 \approx 0.02 \mu\text{m} = 20 \text{ nm}$

Sizes 3d printing (e.g. LPA)

Min, nozzle diameter $0.1 \text{ mm} = 100 \mu\text{m}$

Resolution of printing $0.01 \text{ mm} = 10 \mu\text{m}$

➔ 3d LPA printing is not sufficiently high resolution for fusion target manufacturing. Question, metal 3d printing technology is sufficient?
The nanorod antennas have to be made of gold, aluminum or silver anyway.